ACS APPLIED MATERIALS & INTERFACES

Research Article

www.acsami.org

Self-Assembled Nanocomposite Film with Tunable Enhanced Fluorescence for the Detection of DNA

Xi Zhu,[#] Xiaoyu Wang,[#] Fang He, Fu Tang, and Lidong Li*

School of Materials Science and Engineering, University of Science and Technology Beijing, Beijing 100083, P. R. China

ABSTRACT: In this study, a simple and environmentally friendly, silver nanocomposite film was prepared via the in situ reduction of silver ions in self-assembled chitosan (CS)/sodium alginate film matrixes. Negatively charged DNA containing the fluorescent intercalator acriflavine (Acf) was assembled on the surface of the silver nanocomposite film, to facilitate the detection of DNA. A tunable fluorescence enhancement was achieved for the Acf in the silver nanocomposite film simply by changing the thickness of the interlayer between the DNA and the silver nanocomposite film. Using the interlayer prepared by an assembly of poly(acrylic acid) and CS, a significant enhancement in the fluorescence of Acf was obtained. Owing to the ability of Acf to intercalate into DNA, this hybrid system with an enhanced Acf fluorescence could be used to monitor the template-independent DNA elongation process in a facile, high-efficiency, label-free fashion.

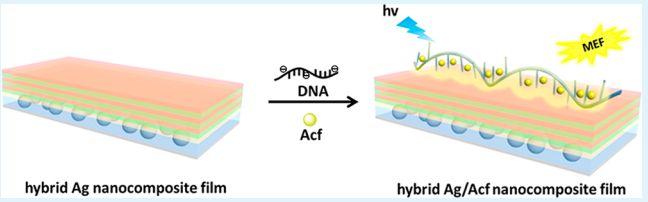

KEYWORDS: *self-assembly, fluorescence, multilayers, nanocomposite, polyelectrolytes, DNA detection*

INTRODUCTION

The detection of fluorescence is an important technique in the chemical and biological fields, because of the high sensitivity and the high efficacy that it is possible to achieve.[1−8] The fluorescent intensity of a fluorophore plays a crucial role in the detection of fluorescence; the sensitivity of detection is related to the fluorescent intensity of a fluorophore. As a result, much effort has been devoted to the modification of fluorophores or the preparation of novel fluorophores, with the aim of obtaining a high fluorescence intensity;[9−12] however, these efforts can be labor intensive and time-consuming. Recently, an efficient method, metal-enhanced fluorescence (MEF), was employed to increase the fluorescence intensity and stability of fluorophores.[13−15]

MEF typically occurs as a result of the near-field interaction of excited fluorescence with surface plasmon resonance (SPR) from adjacent metallic nanostructures.[16,17] To produce MEF, therefore, a suitable metallic nanostructure that supports SPR should be fabricated first. In MEF studies, nanostructured Ag is typically applied as the metallic nanostructure, because of its intense SPR.[18−24] Nanostructured Ag can be prepared via the reduction of Ag ions in the presence of surfactants or polymeric matrixes.[25−27] Layer-by-layer (LbL) multilayer films, which can act as good matrixes for the in situ formation of metal nanoparticles, have attracted much attention.[28−30] The polyelectrolyte components in LbL multilayer films can provide abundant binding sites for Ag ions. Nanostructured Ag films that induce MEF have thus been fabricated in an in situ fashion via the selection of appropriate polyelectrolytes with reducing abilities.[31,32] The magnitude of the effect of MEF on nanostructured Ag film surfaces is distance dependent.[33−36] LbL multilayer films, whose thickness can be accurately controlled,[37−39] can be used to fine-tune the distance between the fluorophores and the metal nanostructures; controllable MEF effects could therefore be realized easily using the self-assembly technique.

DNA polymerase-catalyzed DNA synthesis is an important process in replicating, recombining, and repairing DNA.[40,41] As a template-independent DNA polymerase, terminal deoxynucleotidyl transferase (TdT) can add random nucleotides to single-stranded DNA to form random genes, a process that is meaningful for genomic immunoassays;[42−44] it is therefore necessary to be able to monitor the TdT-catalyzed DNA elongation process. Compared with traditional gel electrophoresis, the detection of DNA on solid surfaces has become increasingly important, because of the advantages of these techniques in terms of their high efficiency and good stability.[45−47] It is therefore desirable to develop new solid detection platforms to meet the demand for DNA detection.

Here, we report a simple and environmentally friendly, hybrid Ag nanocomposite film for the enhancement of the fluorescence of the DNA-intercalated dye acriflavine (Acf),[48−50] an enhancement that allowed the detection of DNA. A hybrid Ag nanocomposite film was prepared via the in situ reduction of Ag ions in polyelectrolytes matrixes, which were prepared via the self-assembly of chitosan (CS) and sodium alginate (ALG). ALG was used as both the reducing and stabilizing agent, so no further external agent was needed. Negatively charged DNA containing Acf, which was intercalated into the DNA, was assembled on the film surface, to allow the detection of DNA. It was easy to adjust the interaction distance between the DNA and the Ag nanocomposite film using biocompatible poly-

Received: November 6, 2014
Accepted: December 25, 2014
Published: December 25, 2014

DOI: 10.1021/am507772e
ACS Appl. Mater. Interfaces 2015, 7, 1334−1339

Scheme 1. Schematic of the Process Used for the Fabrication of the System Platform and the Chemical Structures of the Polyelectrolytes and the Acf

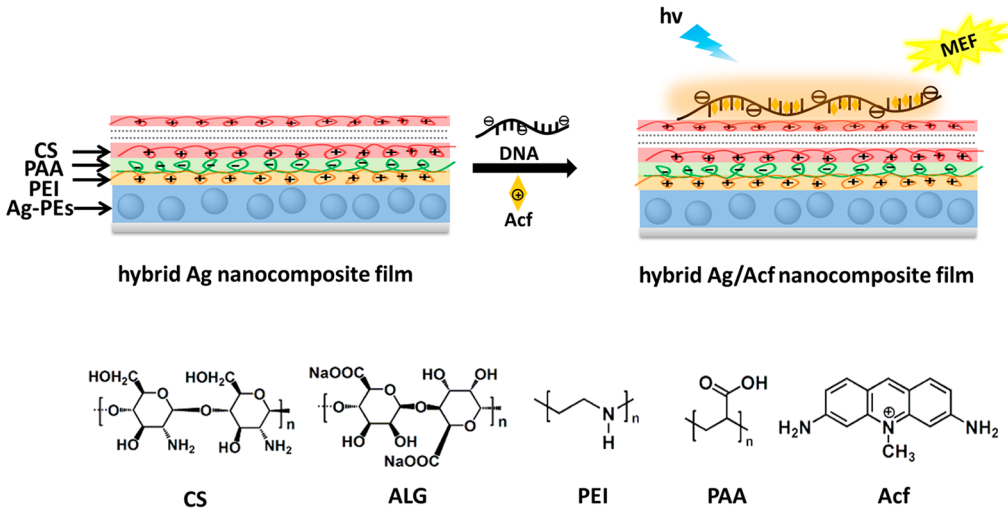

(acrylic acid) (PAA)/CS multilayers, and the MEF effects of the nanocomposite film on the Acf were controlled by varying the thickness of the multilayer. By measuring the enhanced fluorescence intensity of the Acf, the hybrid system could be used to monitor the TdT-catalyzed DNA elongation process with improved simplicity and efficiency.

EXPERIMENTAL METHODS

Materials and Measurements. CS, ALG, PAA (35 wt % aqueous solution, M_r = 30 000), polyethylenimine (PEI, 50 wt % aqueous solution, M_r = 55 000), and Acf were purchased from Sigma-Aldrich. Silver nitrate ($AgNO_3$), ammonium hydroxide solution ($NH_3{\cdot}H_2O$, 25%), and other chemicals and solvents were purchased from Beijing Chemical Reagent Co. Ltd. and were used without further purification. The oligonucleotides were purchased from Shanghai Sangon (Shanghai, China). The DNA concentrations were determined by measuring the absorbance at 260 nm. GoldView nucleic acid stain was purchased from Beijing SBS Genetech Co., Ltd. TdT and dNTPs were obtained from Takara Corporation. Ultraviolet−visible absorption spectra were recorded on a Hitachi U3900 spectrophotometer. The fluorescence spectra were recorded on a Hitachi F-7000 spectrophotometer under xenon lamp excitation. The morphology of the Ag nanoparticles in the films was determined using scanning electron microscopy (SEM, JEOL JSM-7401F). The thickness of each multilayer film was determined using a surface profilometer (XP-2, Ambios Technology, Santa Cruz, CA, USA) at room temperature. Electrophoresis analysis experiments were performed by loading different DNA samples onto a 3% agarose gel stained with GoldView. The gel was run at 80 V for 10 min in a 1× TBE buffer (8.9 mmol/L tris base, 8.9 mmol/L boric acid, 0.2 mmol/L EDTA, pH 7.9). A photograph was taken using a Molecular Imager ChemiDocXRS system.

Preparation of Hybrid Ag Nanocomposite Films. Quartz slides (10 mm × 30 mm) were cleaned via immersion in piranha solution (H_2O_2/H_2SO_4 = 1:3 v/v) for 30 min. *(CAUTION: "Piranha" solution reacts violently with organic materials; it must be handled with extreme care.)* The quartz slides were then washed three times with deionized water under sonication and dried under a gentle stream of nitrogen. Four bilayers of polyelectrolyte CS and ALG films were prepared by alternately immersing the slides in oppositely charged CS (3 mL, 1 mg/mL in 0.1 mol/L acetic acid) and ALG (3 mL, 1 mg/mL) solutions under the same conditions. The outermost layer of the CS/ALG multilayer films was ALG, to allow for the adsorption of Ag ions. Prior to the preparation of the Ag nanoparticles, a silver ammonia solution ($Ag(NH_3)_2OH$) was prepared, as follows: a 2% $NH_3{\cdot}H_2O$ aqueous solution was slowly dropped into 15 mL of a 25 mmol/L $AgNO_3$ solution until the mixture became colorless. The CS/ALG multilayer-coated quartz slides were then immersed in an $Ag(NH_3)_2OH$ solution at 80 °C for 1 h to reduce the $[Ag(NH_3)_2]^+$ ions. By this method, the hybrid Ag nanocomposite films were obtained.

Preparation of Ag/Acriflavine Nanocomposite Films. The hybrid Ag nanocomposite films (ALG-covered) were immersed in a PEI solution (3 mL, 1 mg/mL) for 10 min and then alternately immersed in oppositely charged PAA (3 mL, 1 mg/mL) and CS (3 mL, 1 mg/mL in 0.1 mol/L acetic acid) solutions under the same conditions. In the experiments, one to four bilayers were prepared to control the thickness of the interlayer films. The CS-covered surface was allowed to adsorb the negatively charged DNA. Fifty microliters of a mixture of DNA (1×10^{-6} mol/L) and Acf (1.5×10^{-5} mol/L) was spread on each of the prepared films and then left for 1 h. The slides were then rinsed using PBS buffer (25 mmol/L, pH 7.4) and dried under a gentle stream of nitrogen. As a control, the quartz slides were covered with the same interlayers. The MEF was measured by comparing the fluorescence intensities of the different samples.

Detection of DNA on Ag/Acriflavine Nanocomposite Films. Forty microliters of DNA P11 (1×10^{-5} mol/L), 20 μL of a 5× TdT buffer, 10 μL of a 0.1% BSA suspension, 10 μL of the dNTPs (1×10^{-5} mol/L), 8 μL of TdT (14 U/μL), and 12 μL of deionized water were mixed in solution and then incubated at 37 °C for 10−60 min. At 10, 20, 30, 45, and 60 min, 50 μL of a mixture of the obtained DNA (1×10^{-6} mol/L) and Acf (1.5×10^{-5} mol/L) was separately spread on each prepared film and left for 1 h. The slides were then rinsed using PBS buffer (25 mmol/L, pH 7.4) and dried under a gentle stream of nitrogen.

RESULTS AND DISCUSSION

Preparation and Characterization of Hybrid Ag Nanocomposite Films. The MEF platform system was fabricated using the process illustrated in Scheme 1. First, four layers of the flexible polyelectrolytes CS and ALG were self-assembled on a quartz substrate, to produce a nanoreactor for the preparation of the Ag nanoparticles (Ag NPs). Silver ions were adsorbed on the top anionic ALG layer and then reduced in situ by the aldehyde groups of the ALG (which acted as a reducing agent), forming an Ag-PE film.[51] A thin layer of cationic PEI was then deposited, to improve the self-assembly ability of the structure. Anionic polyelectrolyte PAA and cationic polyelectrolyte CS were deposited stepwise via

DOI: 10.1021/am507772e
ACS Appl. Mater. Interfaces 2015, 7, 1334−1339

self-assembly, to form an interlayer. Finally, negatively charged DNA with fluorescent Acf, which intercalated into the DNA, was deposited on the multilayer films, to allow the assessment of the MEF.

The Ag NPs were synthesized in situ in the CS/ALG multilayer film, using the biopolymer ALG as both a reducing and stabilizing agent. ALG contains not only negative carboxyl groups that can adsorb Ag ions but also aldehyde groups that can act as a reducing agent to reduce Ag ions into Ag NPs.[52] No further external agent was added. The presence of Ag NPs in the CS/ALG multilayer film was confirmed using ultraviolet−visible absorption spectroscopy. As shown in Figure 1,

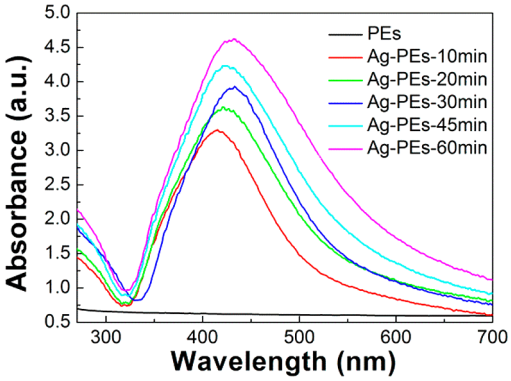

Figure 1. Ultraviolet-visisble absorption spectra for the Ag NPs in the Ag-PE film, shown for different reaction times (10−60 min).

when the reaction time reached 10 min, the Ag NPs exhibited a characteristic absorption peak at approximately at 416 nm, which was consistent with the SPR band of Ag NPs.[53] As the reaction time increased from 10 to 60 min, the intensity of the SPR band increased, indicating the continuous reduction of silver ions. Simultaneously, the maximum in the absorption of the Ag NPs shifted from 416 to 433 nm, which revealed the growth of the Ag NPs.[54,55] The reaction could also be easily visualized through the color changes in the Ag-PE film (from transparent to deep brown).

SEM images of the Ag-PE film taken after different reaction times are shown in Figure 2. The Ag NPs were uniformly and randomly distributed in all of the multilayer films. As the reaction time increased to 60 min, the Ag NPs gradually spread over the surface, and the Ag NPs became larger, results that corresponded to the findings from the ultraviolet−visible spectra. The diameter of the Ag NPs obtained after 60 min was approximately 57 nm, as shown in Figure 2c, a size that was suitable for the generation of MEF effects.[54] Dense Ag structures result in efficient MEF effects;[36] therefore, the 60 min Ag-PE film was selected as the metallic substrate to be used in our study.

MEF Effects of an Ag/Acriflavine Nanocomposite Film. To enhance the fluorescence intensity of fluorophores using the obtained Ag-PE film, it was crucial to consider the distance between the Ag-PE film and the fluorophores. Acf was chosen as the fluorophore, because its absorption spectrum overlapped well with the absorption spectrum of the Ag in the Ag-PE film, which indicated that it would promote MEF (Figure 3).[56,57] Moreover, Acf can intercalate into DNA.[48−50] DNA, which has multiple charges, could be easily assembled on the polyelectrolyte surface.

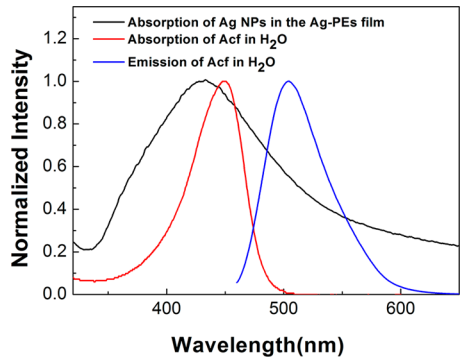

Figure 3. Normalized absorption spectrum (black) of Ag NPs in the Ag-PE film; normalized absorption (red) and fluorescence spectra (blue) of Acf in water upon excitation at 450 nm.

The fluorescence intensity of Acf at different distances from the surface of the Ag-PE film was studied. A series of PEI/$(PAA/CS)_n$ (n = 0−4) interlayers with different thicknesses were prepared via self-assembly, using electrostatic interactions. As shown in Figure 4a, the fluorescence intensity of Acf changed significantly with distance. When the number of PAA/CS bilayers was increased from one to three, the fluorescence intensity of Acf exhibited a significant increase. When the interlayer was formed from three bilayers, the fluorescence intensity of Acf reached its maximum. Further increases in the number of PAA/CS bilayers caused the fluorescence intensity of the Acf to decrease. The thickness of the interlayer was proportional to the number of PAA/CS bilayers, and the thickness of each PAA/CS bilayer was approximately 3.4 nm. The $(PAA/CS)_3$ interlayer produced the largest MEF effect, so the optimal interaction distance in our MEF system was determined to be approximately 10.2 nm.

The adsorption of P11(Acf) was further illustrated in the absorption spectra shown in Figure 4b. After the mixture of DNA P11 and Acf was spread on the prepared film, the absorption spectra (Figure 4b) showed a distinct absorbance peak at 260 nm, which was attributed to the DNA. However, the absorption peak for the Ag NPs was red-shifted from 433 to 444 nm after the assembly of the PEI/$(PAA/CS)_3$ multilayer

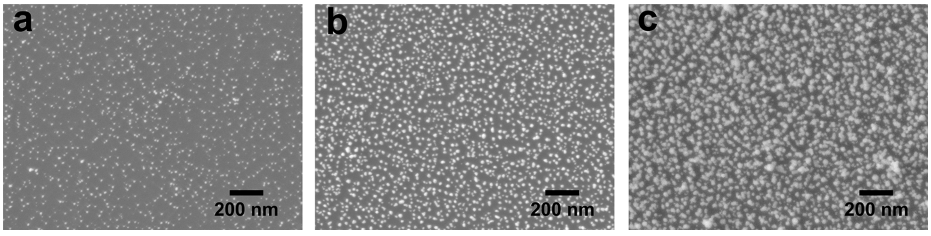

Figure 2. TEM image of the Ag-PE film after different reaction times: (a) 10 min, (b) 30 min, and (c) 60 min.

DOI: 10.1021/am507772e
ACS Appl. Mater. Interfaces 2015, 7, 1334−1339

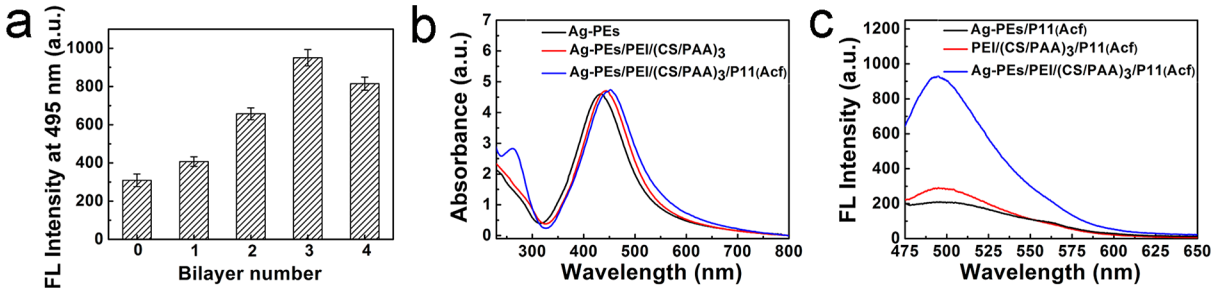

Figure 4. (a) The effect of interlayer thickness on the fluorescence intensity of Acf in an Ag/acriflavine nanocomposite film; (b) ultraviolet−visible absorption spectra for Ag-PEs, Ag-PEs/PEI/$(PAA/CS)_3$, and Ag-PEs/PEI/$(PAA/CS)_3$/P11(Acf) film, and (c) fluorescence spectra for Acf on different substrates. The excitation wavelength was 450 nm. The error bars show the standard deviation determined from three independent measurements.

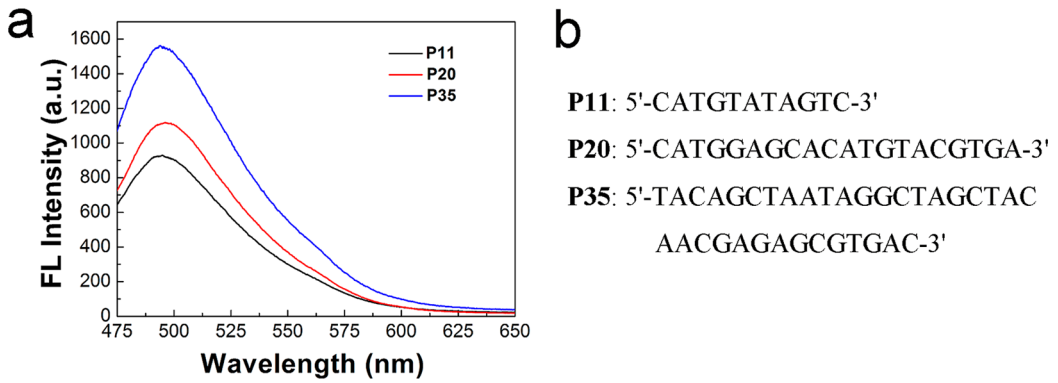

Figure 5. (a) Fluorescence spectra of Acf on the Ag-PEs/PEI/$(PAA/CS)_3$/DNA(Acf) film in the presence of DNA with different base lengths. (b) Sequences of DNA with 11, 20, and 35 bases. The excitation wavelength was 450 nm.

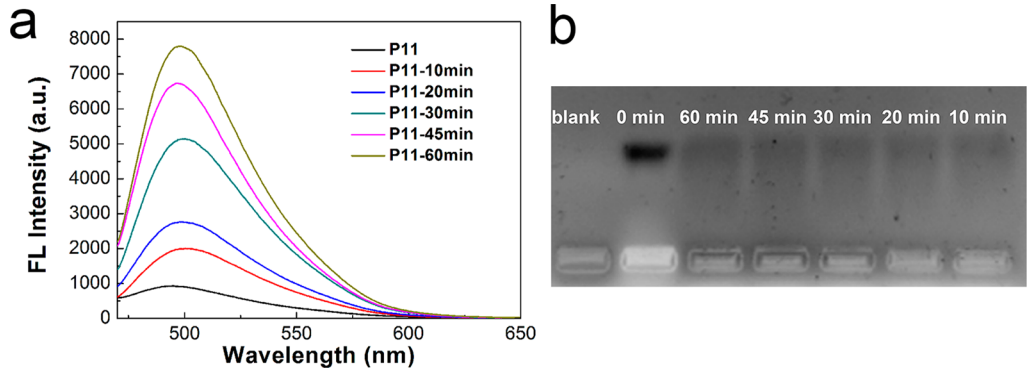

Figure 6. (a) Fluorescence spectra for Acf on the Ag-PEs/PEI/$(PAA/CS)_3$/DNA(Acf) film as a function of the TdT incubation time. (b) Electrophoretic analysis of P11 as a function of the TdT incubation time. [P11] = 4×10^{-6} mol/L.

film and further to 452 nm after the assembly of P11(Acf). The band for Acf at 450 nm overlapped with the absorption peak for Ag. Previous studies demonstrated that the SPR of Ag NPs was affected by the dielectric properties of the surrounding medium.[34,35] This red-shift was therefore likely mainly related to the change in the dielectric environment; this phenomenon also demonstrated the successful assembly of the PEI/$(PAA/CS)_3$/P11(Acf) multilayer film on the Ag-PE film.

The fluorescence spectra for a PEI/$(PAA/CS)_3$/P11(Acf) film without any Ag nanostructures were measured as a control experiment. As shown in Figure 4c, a large, 3.4-fold enhancement was observed for Acf on the Ag-PEs/PEI/$(PAA/CS)_3$/P11(Acf) film, compared with the PEI/$(PAA/CS)_3$/P11(Acf) film. However, the fluorescence intensity of the Acf decreased when the P11(Acf) was directly attached on the Ag-PE film, which proved that an appropriate interlayer was required in the MEF system. The prepared Ag-PE film could be used as a metallic substrate to realize MEF, and the fluorescent properties of the Acf on this substrate were significantly modified.

Detection of DNA Elongation on an Ag/Acriflavine Nanocomposite Film. Taking advantage of the enhanced fluorescence intensity produced in the Acf, we examined the ability of this hybrid system to monitor the template-independent DNA elongation process. First, fluorescence spectra were measured for Acf on the Ag-PEs/PEI/$(PAA/CS)_3$/DNA(Acf) films in the presence of DNA with different base lengths (Figure 5a). The sequences of the DNA strands used are shown in Figure 5b. The fluorescence intensity of the

DOI: 10.1021/am507772e
ACS Appl. Mater. Interfaces 2015, 7, 1334−1339

Acf increased with increasing DNA length, indicating that more of the Acf was intercalated in the DNA that had more bases.

The Ag-PEs/PEI/$(PAA/CS)_3$/DNA(Acf) film was applied to monitor the elongation of DNA by TdT. DNA P11 with 11 bases was used as a primer in the DNA elongation process,[40,58] and TdT then added nucleotides to P11, forming longer DNA strands. The obtained DNA solution was mixed with Acf and then spread on the Ag-PEs/PEI/$(PAA/CS)_3$ film, which was then rinsed with PBS buffer (25 mM, pH 7.4). Figure 6a shows the fluorescence spectra for Acf as a function of the TdT incubation time on the hybrid film. When the incubation time was increased from 0 to 60 min, the fluorescence intensity of Acf increased gradually, indicating that more of the Acf was intercalated in the DNA. Therefore, the DNA with more bases was obtained, and the DNA elongation had occurred. The elongation of P11 was also confirmed using electrophoresis analysis experiments, using a 3% agarose gel (Figure 6b). A solution without P11 was used as a control; in the gel image, this sample is shown in lane 1, and no band was observed. When the incubation time was 0 min, a single band corresponding to P11 was observed in lane 2. When the incubation time was increased, a series of bands was observed in lanes 3−7. More bands appeared with increasing incubation time. The gradually appearing bands indicated that the DNA that had more bases was obtained, and the P11 primer was elongated by TdT. The results were corresponding with the fluorescence spectra shown in Figure 6a. Therefore, in contrast with gel electrophoresis, the hybrid system described here allowed the template-independent, TdT-produced, DNA elongation process to be monitored in a fast, simple, and label-free fashion.

CONCLUSION

A simple, environmentally friendly, Ag nanocomposite film was prepared to enhance the fluorescence intensity of the DNA-intercalated dye Acf. Biocompatible ALG functioned as reductant and stabilizing agent in the in situ synthesis of Ag NPs in CS/ALG multilayer films to form an Ag nanocomposite film. Negatively charged DNA containing the intercalator Acf was adsorbed on the film surface to facilitate the detection of DNA. By varying the distance between the DNA and the Ag nanocomposite film, the Ag nanocomposite film could be used to tunably enhance the fluorescence of the Acf. The conventional self-assembly of PAA and CS was successfully used to produce a 3.4-fold increase in the fluorescence intensity of Acf. When the enhanced fluorescence intensity of the intercalated Acf was exploited, the hybrid system was used to monitor the template-independent, TdT-catalyzed elongation of DNA in a facile, highly efficient, and label-free way.

AUTHOR INFORMATION

Corresponding Author

*Fax: +86 10 82375712. E-mail: lidong@mater.ustb.edu.cn.

Author Contributions

#X.Z. and X.W. contributed equally to this study.

Notes

The authors declare no competing financial interest.

ACKNOWLEDGMENTS

This work was supported by the National Natural Science Foundation of China (51373022), Research Fund for the Doctoral Program of Higher Education of China (20130006110007), and the Program for Chang Jiang Scholars and Innovative Research Team in University. We are grateful to Dr. Libing Liu and Ms. Pengbo Zhang for their helpful suggestions for the electrophoresis analysis experiments.

REFERENCES

(1) Chan, W. C. W.; Nie, S. Quantum Dot Bioconjugates for Ultrasensitive Nonisotopic Detection. *Science* **1998**, *281*, 2016−2018.
(2) Thomas, S. W., III; Joly, G. D.; Swager, T. M. Chemical Sensors Based on Amplifying Fluorescent Conjugated Polymers. *Chem. Rev.* **2007**, *107*, 1339−1386.
(3) Zhu, C.; Liu, L.; Yang, Q.; Lv, F.; Wang, S. Water-Soluble Conjugated Polymers for Imaging, Diagnosis, and Therapy. *Chem. Rev.* **2012**, *112*, 4687−4735.
(4) Fan, C.; Plaxco, K. W.; Heeger, A. J. High-Efficiency Fluorescence Quenching of Conjugated Polymers by Proteins. *J. Am. Chem. Soc.* **2002**, *124*, 5642−5643.
(5) Parthasarathy, A.; Ahn, H.-Y.; Belfield, K. D.; Schanze, K. S. Two-Photon Excited Fluorescence of a Conjugated Polyelectrolyte and Its Application in Cell Imaging. *ACS Appl. Mater. Interfaces* **2010**, *2*, 2744−2748.
(6) Jaiswal, J. K.; Mattoussi, H.; Mauro, J. M.; Simon, S. M. Long-Term Multiple Color Imaging of Live Cells Using Quantum Dot Bioconjugates. *Nat. Biotechnol.* **2002**, *21*, 47−51.
(7) He, Y.; Kang, Z.-H.; Li, Q.-S.; Tsang, C. H. A.; Fan, C.-H.; Lee, S.-T. Ultrastable, Highly Fluorescent, and Water-Dispersed Silicon-Based Nanospheres as Cellular Probes. *Angew. Chem., Int. Ed.* **2009**, *48*, 128−132.
(8) Yuan, H.; Wang, B.; Lv, F.; Liu, L.; Wang, S. Conjugated-Polymer-Based Energy-Transfer Systems for Antimicrobial and Anticancer Applications. *Adv. Mater.* **2014**, *26*, 6978−6982.
(9) Larson, D. R.; Zipfel, W. R.; Williams, R. M.; Clark, S. W.; Bruchez, M. P.; Wise, F. W.; Webb, W. W. Water-Soluble Quantum Dots for Multiphoton Fluorescence Imaging in Vivo. *Science* **2003**, *300*, 1434−1436.
(10) Duan, X.; Liu, L.; Feng, F.; Wang, S. Cationic Conjugated Polymers for Optical Detection of DNA Methylation, Lesions, and Single Nucleotide Polymorphisms. *Acc. Chem. Res.* **2010**, *43*, 260−270.
(11) Jiang, H.; Taranekar, P.; Reynolds, J. R.; Schanze, K. S. Conjugated Polyelectrolytes: Synthesis, Photophysics, and Applications. *Angew. Chem., Int. Ed.* **2009**, *48*, 4300−4316.
(12) Nolan, E. M.; Lippard, S. J. Small-Molecule Fluorescent Sensors for Investigating Zinc Metalloneurochemistry. *Acc. Chem. Res.* **2009**, *42*, 193−203.
(13) Cui, Q.; He, F.; Li, L.; Möhwald, H. Controllable Metal-Enhanced Fluorescence in Organized Films and Colloidal System. *Adv. Colloid Interface Sci.* **2014**, *207*, 164−177.
(14) Aslan, K.; Geddes, C. D. Metal-Enhanced Chemiluminescence: Advanced Chemiluminescence Concepts for the 21st Century. *Chem. Soc. Rev.* **2009**, *38*, 2556−2564.
(15) Aslan, K.; Gryczynski, I.; Malicka, J.; Matveeva, E.; Lakowicz, J. R.; Geddes, C. D. Metal-Enhanced Fluorescence: An Emerging Tool in Biotechnology. *Curr. Opin. Biotechnol.* **2005**, *16*, 55−62.
(16) Geddes, C. D.; Lakowicz, J. R. Editorial Metal-Enhanced Fluorescence. *J. Fluoresc.* **2002**, *12*, 121−129.
(17) Fort, E.; Grésillon, S. Surface Enhanced Fluorescence. *J. Phys. D: Appl. Phys.* **2008**, *41*, 013001.
(18) Aslan, K.; Wu, M.; Lakowicz, J. R.; Geddes, C. D. Fluorescent Core-Shell Ag@SiO_2 Nanocomposites for Metal-Enhanced Fluorescence and Single Nanoparticle Sensing Platforms. *J. Am. Chem. Soc.* **2007**, *129*, 1524−1525.
(19) Tang, F.; He, F.; Cheng, H.; Li, L. Self-Assembly of Conjugated Polymer-Ag@SiO_2 Hybrid Fluorescent Nanoparticles for Application to Cellular Imaging. *Langmuir* **2010**, *26*, 11774−11778.
(20) Viger, M. L.; Live, L. S.; Therrien, O. D.; Boudreau, D. Reduction of Self-Quenching in Fluorescent Silica-Coated Silver Nanoparticles. *Plasmonics* **2008**, *3*, 33−40.

DOI: 10.1021/am507772e
ACS Appl. Mater. Interfaces 2015, 7, 1334−1339

(21) Neal, T. D.; Okamoto, K.; Scherer, A. Surface Plasmon Enhanced Emission from Dye Doped Polymer Layers. *Opt. Express* **2005**, *13*, 5522−5527.
(22) Fu, Y.; Zhang, J.; Lakowicz, J. R. Largely Enhanced Single-Molecule Fluorescence in Plasmonic Nanogaps Formed by Hybrid Silver Nanostructures. *Langmuir* **2013**, *29*, 2731−2738.
(23) Zhang, J.; Ray, K.; Fu, Y.; Lakowicz, J. R. First Observation of Enhanced Luminescence from Single Lanthanide Chelates on Silver Nanorods. *Chem. Commun.* **2014**, *50*, 9383−9386.
(24) Zhang, Y.; Mali, B. L.; Aitken, C.; Geddes, C. D. Highly Sensitive Quantitation of Human Serum Albumin in Clinical Samples for Hypoproteinemia Using Metal-Enhanced Fluorescence. *J. Fluoresc.* **2013**, *23*, 187−192.
(25) Xu, H.; Suslick, K. S. Water-Soluble Fluorescent Silver Nanoclusters. *Adv. Mater.* **2010**, *22*, 1078−1082.
(26) Antonietti, M.; Gröhn, F.; Hartmann, J.; Bronstein, L. Nonclassical Shapes of Noble-Metal Colloids by Synthesis in Microgel Nanoreactors. *Angew. Chem., Int. Ed.* **1997**, *36*, 2080−2083.
(27) Zhang, J.; Xu, S.; Kumacheva, E. Polymer Microgels: Reactors for Semiconductor, Metal, and Magnetic Nanoparticles. *J. Am. Chem. Soc.* **2004**, *126*, 7908−7914.
(28) Wang, T. C.; Rubner, M. F.; Cohen, R. E. Polyelectrolyte Multilayer Nanoreactors for Preparing Silver Nanoparticle Composites: Controlling Metal Concentration and Nanoparticle Size. *Langmuir* **2002**, *18*, 3370−3375.
(29) Shi, X.; Shen, M.; Möhwald, H. Polyelectrolyte Multilayer Nanoreactors toward the Synthesis of Diverse Nanostructured Materials. *Prog. Polym. Sci.* **2004**, *29*, 987−1019.
(30) Dai, J.; Bruening, M. L. Catalytic Nanoparticles Formed by Reduction of Metal Ions in Multilayered Polyelectrolyte Films. *Nano Lett.* **2002**, *2*, 497−501.
(31) Joly, S.; Kane, R.; Radzilowski, L.; Wang, T.; Wu, A.; Cohen, R. E.; Thomas, E. L.; Rubner, M. F. Multilayer Nanoreactors for Metallic and Semiconducting Particles. *Langmuir* **2000**, *16*, 1354−1359.
(32) Tong, L.; Ma, N.; Tang, F.; Qiu, D.; Cui, Q.; Li, L. pH- and Thermoresponsive Ag/Polyelectrolyte Hybrid Thin Films for Tunable Metal-Enhanced Fluorescence. *J. Mater. Chem.* **2012**, *22*, 8988−8993.
(33) Ray, K.; Badugu, R.; Lakowicz, J. R. Langmuir-Blodgett Monolayers of Long-Chain NBD Derivatives on Silver Island Films: Well-Organized Probe Layer for the Metal-Enhanced Fluorescence Studies. *J. Phys. Chem. B* **2006**, *110*, 13499−13507.
(34) Cui, Q.; He, F.; Wang, X.; Xia, B.; Li, L. Gold Nanoflower@Gelatin Core-Shell Nanoparticles Loaded with Conjugated Polymer Applied for Cellular Imaging. *ACS Appl. Mater. Interfaces* **2013**, *5*, 213−219.
(35) Wang, X.; He, F.; Zhu, X.; Tang, F.; Li, L. Hybrid Silver Nanoparticle/Conjugated Polyelectrolyte Nanocomposites Exhibiting Controllable Metal-Enhanced Fluorescence. *Sci. Rep.* **2014**, *4*, 4406.
(36) Ma, N.; Tang, F.; Wang, X.; He, F.; Li, L. Tunable Metal-Enhanced Fluorescence by Stimuli-Responsive Polyelectrolyte Interlayer Films. *Macromol. Rapid Commun.* **2011**, *32*, 587−592.
(37) Decher, G. Fuzzy Nanoassemblies: Toward Layered Polymeric Multicomposites. *Science* **1997**, *277*, 1232−1237.
(38) Lvov, Y.; Decher, G.; Sukhorukov, G. Assembly of Thin Films by Means of Successive Deposition of Alternate Layers of DNA and Poly(ally1amine). *Macromolecules* **1993**, *26*, 5396−5399.
(39) Alvarez-Puebla, R. A.; dos Santos, D. S., Jr.; Aroca, R. F. SERS Detection of Environmental Pollutants in Humic Acid-Gold Nanoparticle Composite Materials. *Analyst* **2007**, *132*, 1210−1214.
(40) Fowler, J. D.; Suo, Z. Biochemical, Structural, and Physiological Characterization of Terminal Deoxynucleotidyl Transferase. *Chem. Rev.* **2006**, *106*, 2092−2110.
(41) Benedict, C. L.; Gilfillan, S.; Thai, T.-H.; Kearney, J. F. Terminal Deoxynucleotidyl Transferase and Repertoire Development. *Immunol. Rev.* **2000**, *175*, 150−157.
(42) Hübscher, U.; Maga, G.; Spadari, S. Eukaryotic DNA Polymerases. *Annu. Rev. Biochem.* **2002**, *71*, 133−163.
(43) Friedberg, E. C.; Feaver, W. J.; Gerlach, V. L. The Many Faces of DNA Polymerases: Strategies for Mutagenesis and for Mutational Avoidance. *Proc. Natl. Acad. Sci. U. S. A.* **2000**, *97*, 5681−5683.
(44) Andrade, P.; Martín, M. J.; Juárez, R.; de Saro, F. L.; Blanco, L. Limited Terminal Transferase in Human DNA Polymerase Defines the Required Balance Between Accuracy and Efficiency in NHEJ. *Proc. Natl. Acad. Sci. U. S. A.* **2009**, *106*, 16203−16208.
(45) Lv, F.; Liu, L.; Wang, S. Signal Amplifying Optical DNA Detection on Solid Support with Fluorescent Conjugated Polymers. *Curr. Org. Chem.* **2011**, *15*, 548−556.
(46) Georganopoulou, D. G.; Chang, L.; Nam, J.-M.; Thaxton, C. S.; Mufson, E. J.; Klein, W. L.; Mirkin, C. A. Nanoparticle-Based Detection in Cerebral Spinal Fluid of a Soluble Pathogenic Biomarker for Alzheimer's Disease. *Proc. Natl. Acad. Sci. U. S. A.* **2005**, *102*, 2273−2276.
(47) Raymond, F. R.; Ho, H.-A.; Peytavi, R.; Bissonnette, L.; Boissinot, M.; Picard, F. J.; Leclerc, M.; Bergeron, M. G. Detection of Target DNA Using Fluorescent Cationic Polymer and Peptide Nucleic Acid Probes on Solid Support. *BMC Biotechnol.* **2005**, *5*, 10.
(48) Carmichael, G. G.; McMaster, G. K. The Analysis of Nucleic Acids in Gels Using Glyoxal and Acridine Orange. *Methods Enzymol.* **1980**, *65*, 380−391.
(49) Bruno, J. C.; Sincock, S. A.; Stopa, P. J. Highly Selective Acridine and Ethidium Staining of Bacterial DNA and RNA. *Biotechnol. Histochem.* **1996**, *71*, 130−136.
(50) Medhi, C.; Mitchell, J. B. O.; Price, S. L.; Tabor, A. B. Electrostatic Factors in DNA Intercalation. *Biopolymers* **1999**, *52*, 84−93.
(51) Xia, B.; Cui, Q.; He, F.; Li, L. Preparation of Hybrid Hydrogel Containing Ag Nanoparticles by a Green in Situ Reduction Method. *Langmuir* **2012**, *28*, 11188−11194.
(52) Sharma, S.; Sanpui, P.; Chattopadhyay, A.; Ghosh, S. S. Fabrication of Antibacterial Silver Nanoparticle-Sodium Alginate-Chitosan Composite Films. *RSC Adv.* **2012**, *2*, 5837−5843.
(53) Hutter, E.; Fendler, J. H. Exploitation of Localized Surface Plasmon Resonance. *Adv. Mater.* **2004**, *16*, 1685−1706.
(54) Yguerabide, J.; Yguerabide, E. E. Light-Scattering Submicroscopic Particles as Highly Fluorescent Analogs and Their Use as Tracer Labels in Clinical and Biological Applications: II. Experimental Characterization. *Anal. Biochem.* **1998**, *262*, 157−176.
(55) Wiley, B. J.; Im, S. H.; Li, Z.-Y.; McLellan, J.; Siekkinen, A.; Xia, Y. Maneuvering the Surface Plasmon Resonance of Silver Nanostructures Through Shape-Controlled Synthesis. *J. Phys. Chem. B* **2006**, *110*, 15666−15675.
(56) Chen, Y.; Munechika, K.; Ginger, D. S. Dependence of Fluorescence Intensity on the Spectral Overlap Between Fluorophores and Plasmon Resonant Single Silver Nanoparticles. *Nano Lett.* **2007**, *7*, 690−696.
(57) Ming, T.; Chen, H.; Jiang, R.; Li, Q.; Wang, J. Plasmon-Controlled Fluorescence: Beyond the Intensity Enhancement. *J. Phys. Chem. Lett.* **2012**, *3*, 191−202.
(58) He, F.; Liu, L.; Li, L. Water-Soluble Conjugated Polymers for Amplified Fluorescence Detection of Template-Independent DNA Elongation Catalyzed by Polymerase. *Adv. Funct. Mater.* **2011**, *21*, 3143−3149.

DOI: 10.1021/am507772e
ACS Appl. Mater. Interfaces 2015, 7, 1334−1339